SIMULATION STUDIES OF AN X-RAY PINHOLE CAMERA FOR THE HALF DIAGNOSTICS BEAMLINE

Xinru-Gao*[1], Yongbin-Leng[1,2]
[1]University of Science and Technology of China, Hefei, China
[2]National Synchrotron Radiation Laboratory(NSRL), Hefei, China

Abstract

The X-ray pinhole camera for the Hefei Advanced Light Facility (HALF) requires a system spatial resolution better than 5 µm to diagnose micrometre-scale electron beams. Analytical models commonly treat the pinhole as an ideal square aperture, assume a Gaussian point spread function (PSF), and employ Fresnel or Fraunhofer diffraction formulas. This work validates these approximations using wave-optics simulations of a realistic thick tungsten pinhole, and evaluates upstream heat load and thermal PSF degradation. Simulations over a wide range of source-to-pinhole and pinhole-to-detector distances confirm that at the multi-metre working distances of HALF the square-aperture and Gaussian-PSF approximations are excellent, and the Fraunhofer formula is sufficient. Thermal analysis for three copper absorber configurations shows that only a deep conical absorber (inspired by the SSRF design) can adequately protect the aluminium window and pinhole. When combined with a 25–30 µm aperture, thermally induced PSF broadening is negligible, preserving near-diffraction-limited imaging and sub-5 µm resolution. These results provide a validated design basis for the HALF X-ray diagnostics beamline.

INTRODUCTION

Transverse beam size is a critical parameter for the Hefei Advanced Light Facility (HALF), a diffraction-limited storage ring requiring micrometre-scale (10–80 µm) diagnostics. X-ray pinhole cameras are widely used due to their non-invasive nature and mechanical simplicity, but achieving the target system resolution of sub-5 µm requires a highly accurate model of the Point Spread Function (PSF) [1, 2].

Analytical models typically rely on three simplifications: (i) treating the pinhole as an ideal thin square aperture, (ii) assuming a Gaussian PSF, and (iii) applying Fresnel or Fraunhofer diffraction formulas [3, 4]. While computationally efficient, these approximations neglect the thickness of realistic tungsten blocks, which may introduce collimation and scattering effects. Quantitative validation of these models across the expected working distances is therefore essential.

Furthermore, the thermal stability of the diagnostic system is a concern. The bending-magnet radiation carries significant power that can cause vacuum window failure and thermal distortion of the pinhole. Various copper absorber designs, including a deep conical scheme inspired by the SSRF design [5], must be evaluated to guarantee safe operation and sub-5 µm resolution. This work systematically validates standard PSF approximations and investigates the thermal performance of different absorber configurations using integrated wave-optics and finite-element simulations, providing a design basis for the HALF diagnostics beamline.

Source Parameters and Simulation Geometry

The X-ray source is a bending magnet (RC07-B5) of the 2.2 GeV HALF storage ring, with critical energy 1.3744 keV. After a 1 mm aluminium window, the effective photon energy is 13.12 keV (wavelength 0.0945 nm) [1].

The pinhole consists of two thick tungsten blocks that form a square aperture. The block thickness provides sufficient attenuation but introduces collimation and small-angle scattering effects absent in ideal thin-aperture models. For PSF validation, upstream components (absorber and window) are omitted to isolate the intrinsic pinhole optics.

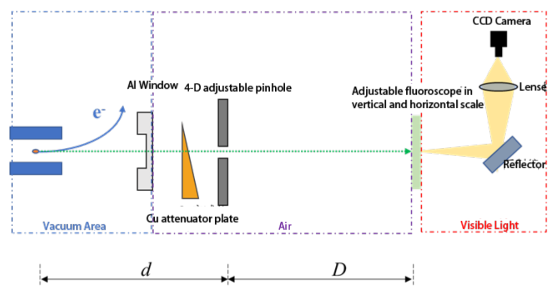

Figure 1: Schematic of the simulation geometry. The distances d (source–pinhole) and D (pinhole–detector) are varied independently.

The geometry is defined by d and D (Fig. 1). A wide parameter sweep explores the near-field to far-field transition. For each (d, D) pair, the detector-plane intensity is computed in the following section. Scattered radiation and finite detector resolution are not considered at this stage; the analysis concentrates on the direct imaging properties of the pinhole.

PSF Models and Validation Metrics

For each (d, D) combination defined in Section just above, the detector-plane intensity distribution is evaluated with four distinct approaches:

1. **Realistic thick pinhole**: full wave-optics simulation of the two-block tungsten assembly (10 mm thickness, 25 µm × 25 µm aperture), capturing collimation and small-angle scattering.
2. **Ideal square aperture**: an infinitesimally thin 25 µm × 25 µm aperture modelled in the same simulation framework.

* gaoxinru@mail.ustc.edu.cn

The validity of the square-aperture approximation is assessed by the two-dimensional correlation coefficient between PSF images computed in models (1) and (2).

Thermal Load and Distortion Simulation

The upstream heat load is evaluated at a plane 6.5 m from the source for three copper absorber configurations:

- **Case A**: no absorber (direct illumination of the aluminium window and tungsten pinhole).
- **Case B**: shallow conical absorber with inlet/outlet diameters of 5 mm/5.7 mm and 20 mm length.
- **Case C**: deep conical absorber inspired by the SSRF design (tapered from 16 mm to 1.6 mm).

The absorbed power density in the aluminium window and the pinhole assembly is computed for each case. For the configuration most representative of the HALF baseline, the resulting temperature distribution is used to calculate the thermal deformation of the pinhole edges. The deformed aperture geometries are imported back into the wave-optics simulation to compute the degraded PSF for pinhole sizes of 15, 20, 25, 30 and 40 µm, with the cold (un-deformed) PSF serving as reference.

SIMULATION RESULTS

Validation of the Square-Aperture Approximation

To quantitatively evaluate the validity of the square-aperture approximation (model (2) in Section "PSF Models and Validation Metrics"), we calculate the two-dimensional Pearson correlation coefficient between the PSF intensity distributions of the realistic thick pinhole (model (1)) and the ideal thin square aperture (model (2)) for every simulated (d, D) pair. The correlation coefficient is defined as

$$\rho = \frac{\sum_{i,j}(I_{1,ij} - \bar{I}_1)(I_{2,ij} - \bar{I}_2)}{\sqrt{\sum_{i,j}(I_{1,ij} - \bar{I}_1)^2}\sqrt{\sum_{i,j}(I_{2,ij} - \bar{I}_2)^2}}, \qquad (1)$$

where I_1 and I_2 denote the two-dimensional PSF arrays, and $\bar{I}_1$, $\bar{I}_2$ their mean values. A correlation $\rho = 1$ would indicate perfect morphological identity between the two PSFs.

Figure 2 shows the resulting correlation map plotted against the distances d (m) and D (m).

The map reveals a systematic trend: for small d and D (compact geometries in the extreme near field) the correlation can drop noticeably below unity due to three-dimensional pinhole effects such as aperture-edge scatter and vignetting. As both d and D increase, ρ rapidly approaches 1. In the region where $d \gtrsim 0.5$ m and $D \gtrsim 0.5$ m, the correlation exceeds 0.98, indicating that the PSF of the thick tungsten pinhole becomes essentially indistinguishable from that of an ideal square aperture. A representative example is the profile for $d = D = 5$ m (Fig. 3), where the two PSFs are practically identical.

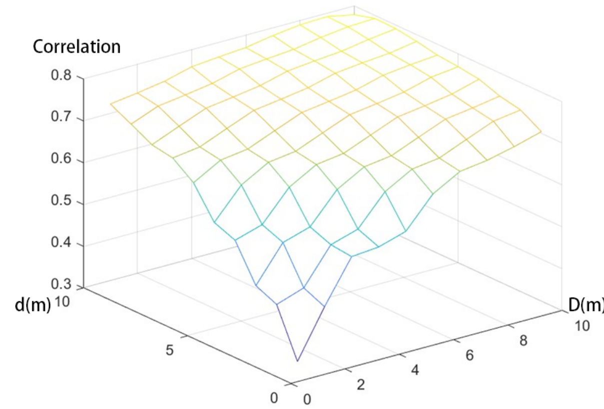

Figure 2: Correlation ρ between the realistic thick-pinhole PSF and the ideal square-aperture PSF as a function of d and D.

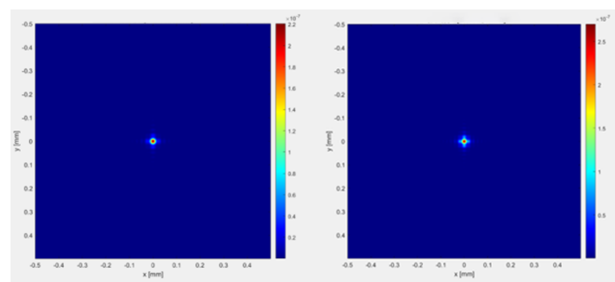

Figure 3: Direct comparison of the two PSF distributions at $d = D = 5$ m, corresponding to the high-correlation region.

For the multi-metre working distances foreseen in the HALF extraction line, both d and D are well above the threshold identified above. The square-aperture approximation is therefore fully justified for analytical and numerical modelling of the pinhole camera PSF, removing the need to simulate the full three-dimensional block geometry in routine beam-size extraction.

Upstream Heat Load and Thermally-Induced PSF Degradation

Upstream Power Density Distribution The absorbed power density in the 1 mm aluminium vacuum window and the tungsten pinhole assembly was evaluated at a plane 6.5 m from the bending-magnet source for the three copper absorber configurations: no absorber (direct illumination), shallow conical absorber (5 mm/5.7 mm inlet/outlet, 20 mm length), deep conical absorber (1 mm/1.6 mm inlet/outlet, 16 mm length, inspired by SSRF), as shown in Fig. 4.

Without a copper absorber (Case A), the direct synchrotron radiation fan deposits a power density exceeding the safe operational threshold, posing a risk of window failure and pinhole damage. The shallow absorber (Case B) reduces the load by a factor of approximately three but still leaves a non-negligible heat load on the downstream components. Only the deep conical design (Case C) brings the absorbed

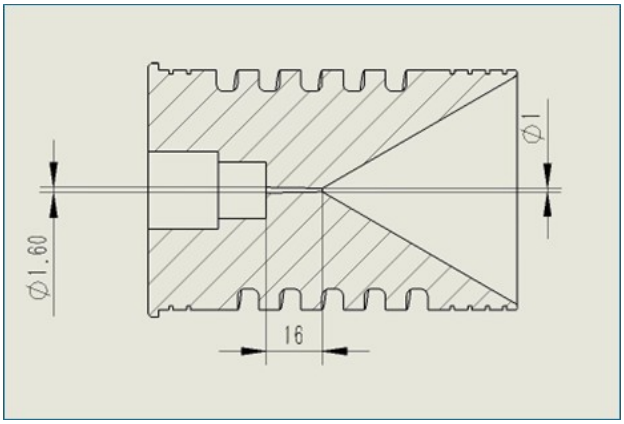

Figure 4: The Cu absorber of the Al window at SSRF [5].

power density well within the acceptable range, protecting both the window and the tungsten aperture.

PSF Degradation due to Thermal Distortion The temperature distribution computed for the Case C configuration was used to determine the thermal deformation of the pinhole edges via simulation analysis. The deformed aperture profiles were then imported into the wave-optics simulation, and the resulting PSFs were compared with the cold (undeformed) PSF for pinhole sizes of 15, 20, 25, 30 and 40 µm.

Figure 5 displays the horizontal PSF profiles for the most critical small apertures (15 µm and 30 µm). As shown in the figure, thermal load exhibits only a minor modification and the profile retains a nearly Gaussian shape. The 25 µm aperture (not shown) behaves similarly to the 30 µm case, with a relative degradation marginal enough to preserve sub-5 µm overall system resolution after deconvolution.

In conclusion, the deep conical copper absorber (Case C) is essential for safe operation of the HALF X-ray pinhole camera and effectively prevents excessive heating of the upstream vacuum window. When combined with a pinhole aperture of 25–30 µm, the thermally-induced PSF degradation is negligible, allowing the imaging system to maintain near-diffraction-limited performance and a spatial resolution well below the 5 µm target. This configuration is therefore recommended as the baseline for the HALF diagnostic beamline.

CONCLUSION

This simulation study validates the optical and thermal design of the HALF X-ray pinhole camera. Wave-optics analysis demonstrates that for multi-metre working distances, the ideal square-aperture and Gaussian-PSF approximations are highly accurate (correlation $\rho > 0.98$), and Fraunhofer diffraction is sufficient for routine beam-size extraction.

Thermal analysis confirms that a deep conical copper absorber is critical to maintaining safe power densities at the aluminium window. Simulations show that for pinhole apertures of 25–30 µm, thermally induced PSF degradation is negligible, ensuring the system meets the sub-5 µm resolution requirement. In contrast, smaller apertures exhibit

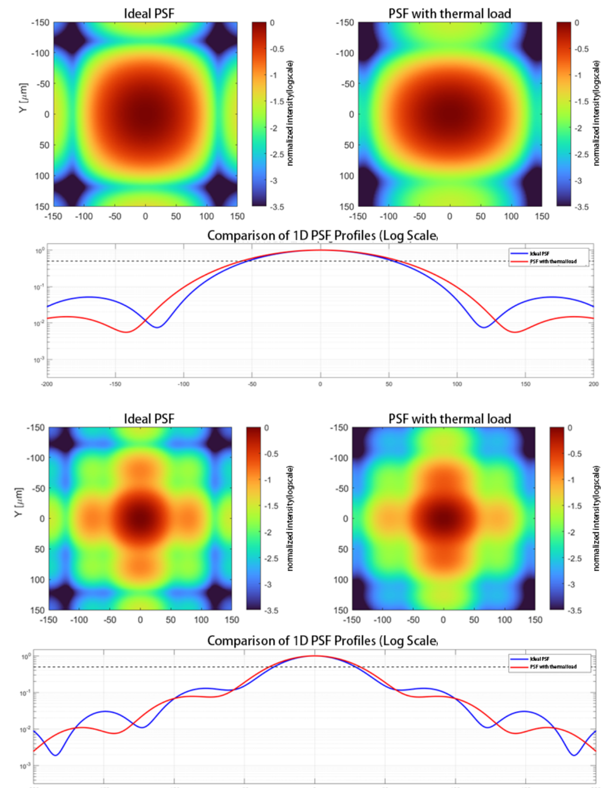

Figure 5: Comparison of cold and thermally-deformed PSF profiles and 1D extraction for pinhole apertures of 15 µm (top) and 30 µm (bottom).

significant thermal broadening. Consequently, the combination of a deep conical absorber and a 25–30 µm aperture is recommended as the baseline configuration for HALF. This validated framework provides a robust reference for the engineering of high-resolution X-ray diagnostics at low-emittance light sources.

REFERENCES

[1] Z. Bai, G. Liu, T. He, *et al.*, "Preliminary physics design of the Hefei Advanced Light Facility storage ring", *High Power Laser Part. Beams*, vol. 34, no. 10, p. 104003, 2022. doi:10.11884/HPLPB202234.220137

[2] C. A. Thomas, G. Rehm, and R. Bartolini, "An X-ray pinhole camera with a range of defined apertures", in *Proc. BIW'12*, Newport News, VA, USA, Apr. 2012, pp. 116–118.

[3] B. Gao *et al.*, "Upgrade of the X-ray pinhole camera system at SSRF", *Nucl. Sci. Tech.*, vol. 29, no. 8, p. 115, 2018. doi:10.1007/s41365-018-0444-7

[4] C. A. Thomas and G. Rehm, "X-ray pinhole camera resolution and emittance measurement", *Phys. Rev. Spec. Top. Accel. Beams*, vol. 13, p. 022805, 2010. doi:10.1103/PhysRevSTAB.13.022805

[5] Y. B. Leng, *et al.*, "Beam based calibration of X-ray pinhole camera in SSRF", *Chin. Phys. C*, vol. 36, no. 1, pp. 80–83, 2012. doi:10.1088/1674-1137/36/1/014